The Phenomenology of Pomeron Enhancement *

E. Gotsman,† E. Levin,‡ U. Maor,§ and J.S. Miller¶

Department of Particle Physics, School of Physics and Astronomy

Raymond and Beverly Sackler Faculty of Exact Science

Tel Aviv University, Tel Aviv, 69978, Israel

Abstract

Multi Pomeron interactions are the main source of high mass diffraction. Their role in high energy dynamics greatly influences the predictions for high energy cross sections and survival probabilities of hard diffraction channels, notably, diffractive Higgs production at the LHC. Our approach, is motivated by the fact that we obtain a very small value for the fitted slope of the Pomeron trajectory, which justifies the use of perturbative QCD for soft scattering. Our suggested model differs from the proposal of the Durham KMR group which is based on a parton model interpretation of the Reggeon calculus in the complex J-plane in which multi Pomeron vertices are arbitrarily defined. The theoretical input and predictions of the two groups, as well as their data analysis and procedures are compared and evaluated.

PACS numbers:

Keywords: Soft Pomeron, Hard Pomeron, Multi Pomerons, Diffraction, Survival Probability.

* Based on a talk by U. Maor at LISHEP 2009, UERJ, Rio de Janeiro, 16-23 Jan. 2009.

†Email: gotsman@post.tau.ac.il

‡Email: leving@post.tau.ac.il

§Email: maor@post.tau.ac.il

¶Email: jeremymi@post.tau.ac.il

I. INTRODUCTION

The purpose of this communication is to discuss the role of multi Pomeron interactions in high energy scattering. Our study is two fold: on the one hand, we wish to assess the relevance of multi Pomeron interactions in the calculation of soft scattering cross sections in the ISR-Tevatron range, for which data is available. Our main goal, though, is to seek conclusive evidence for multi Pomeron interactions at the LHC and Auger. The study we present is essential for realistic estimates of inelastic hard diffraction rates, in particular, central exclusive diffractive Higgs production at the LHC, as it is necessary to have a reliable calculation of the gap survival probability for this process [1]. In the following we discuss and assess the latest versions of two classes of eikonal models:
1) The Tel Aviv (GLMM) group has two publications: GLMM(08)[2] in which our model is presented, detailing our calculation of the enhanced Pomeron diagrams. The theoretical basis of this model is further explored in GLMM(09)[3].
2) The Durham (KMR) group has presented three recent versions of its model: KMR(07)[4], KMR(08)[6] and LKMR(09)[5]. KMR(08) results, spread over six recent publications, are based on KMR(07) with a more detailed parametrization of the Pomeron contribution. LKMR(09)[5] is a more modest model in which high mass diffraction originates exclusively from the leading triple Pomeron diagram with secondary Regge corrections. Although the Tel Aviv and Durham models have a similar philosophy, their formulations, data analysis and predictions differ significantly. In the following we shall discuss the consequences of these differences.

II. GOOD-WALKER EIKONAL MODELS

Current eikonal models are multi channel, including both elastic and diffractive re-scatterings of the initial projectiles[1]. This is a consequence of the Good-Walker (GW) mechanism[7] in which the proton (anti-proton) wave function has elastic and diffractive components. Models based on the GW mechanism reproduce the total and elastic cross sections well, but fail to describe the diffractive cross section data (see Refs.[2, 5, 8]). Theoretically[9], these deficiencies can be eliminated by the introduction of multi Pomeron interactions leading to high mass diffraction. These "Pomeron-enhanced" contributions, are

derived from Gribov's Reggeon calculus[10]. The zero order, on which these calculations are based, is Mueller's triple Pomeron high mass SD formalism[11].

Consider[8] a vertex with an incoming hadron $|h\rangle$ and outgoing diffractive system approximated as a single state $|D\rangle$. The Good-Walker mechanism is based on the observation that these states do not diagonalize the 2×2 interaction matrix. We denote the interaction matrix eigenstates by ψ_1 and ψ_2. The wave functions of the incoming hadron and outgoing diffractive state are

$$\psi_h = \alpha\,\psi_1 + \beta\,\psi_2\,, \tag{II.1}$$

$$\psi_D = -\beta\,\psi_1 + \alpha\,\psi_2\,, \tag{II.2}$$

where, $\alpha^2 + \beta^2 = 1$. For each of the four independent elastic scattering amplitudes $A^S_{i,k}(s,b)$ we write its elastic unitarity equation

$$Im\,A^S_{i,k}(s,b) = |A^S_{i,k}(s,b)|^2 + G^{in}_{i,k}(s,b), \tag{II.3}$$

in which

$$A^S_{i,k}(s,b) = i\left(1 - \exp(-\frac{1}{2}\Omega^S_{i,k}(s,b))\right), \tag{II.4}$$

$$G^{in}_{i,k}(s,b) = (1 - \exp(-\Omega^S_{i,k}(s,b))). \tag{II.5}$$

$G^{in}_{i,k}$ is the summed probability for all non GW induced inelastic final states. From Eq. (II.5) we deduce that $P^S_{i,k}(s,b) = exp(-\Omega^S_{i,k}(s,b))$ is the probability that the GW (i,k) projectiles will reach the final large rapidity gap (LRG) interaction in their initial state, regardless of their prior re-scatterings.

For p-p and $\bar{p}$-p scattering $A^S_{1,2} = A^S_{2,1}$, which reduces the number of independent amplitudes to three. The corresponding elastic, SD and DD amplitudes are

$$a_{el}(s,b) = i\{\alpha^4 A^S_{1,1} + 2\alpha^2\beta^2 A^S_{1,2} + \beta^4 \mathcal{A}^S_{2,2}\}, \tag{II.6}$$

$$a_{sd}(s,b) = i\alpha\beta\{-\alpha^2 A^S_{1,1} + (\alpha^2 - \beta^2)A^S_{1,2} + \beta^2 A^S_{2,2}\}, \tag{II.7}$$

$$a_{dd} = i\alpha^2\beta^2\{A^S_{1,1} - 2A^S_{1,2} + A^S_{2,2}\}. \tag{II.8}$$

For more details see Refs.[1, 2, 8] and references therein.

Eikonal models based on the GW mechanism use a Regge like formalism in which the soft Pomeron trajectory is given by

$$\alpha_{I\!P}(t) = 1 + \Delta_{I\!P} + \alpha'_{I\!P} t. \tag{II.9}$$

The corresponding opacity is

$$\Omega^S_{i,k}(s,b) = \nu^S_{i,k}(s)\Gamma^S_{i,k}(s,b,\alpha'_{I\!P}). \tag{II.10}$$

$\nu^S_{i,k}(s) = g_i g_k (\frac{s}{s_0})^{\Delta_{I\!P}}$ and $\Gamma^S_{i,k}$ are the b-space profiles. The profiles are constructed so as to reproduce the differential cross sections. The normalization and constraints on the large b behaviour of the profiles, are determined from the data analysis.

In GLMM(08,09) an (i,k) b-profile is given as the b-transform of a two pole t-profile ($t=-q^2$). Setting $\alpha'_{I\!P}$= 0, the profiles are energy independent,

$$\frac{1}{(1\ +\ q^2/m_i^2)^2} \times \frac{1}{(1\ +\ q^2/m_k^2)^2} \implies \Gamma\left(b; m_i, m_k; \alpha'_{I\!P}=0\right). \tag{II.11}$$

A small energy dependence is introduced via

$$m_i^2 \implies m_i^2(s) \equiv \frac{m_i^2}{1\ +\ \alpha'_{I\!P}\ln(s/s_0)/4m_i^2}. \tag{II.12}$$

The above parametrization is compatible with the requirements of analyticity/crossing symmetry at large b, pQCD at large q^2 and Regge at small t. For details see Ref.[3].

Models in which diffraction is exclusively given by the GW mechanism, were studied by GLMM(08) and LKMR(09). KMR(07,08) do not discuss a GW model on its own. This was considered in an earlier publication[12] denoted KMR(00). GLMM(08) fitted Pomeron parameters for its GW model are presented in Table I. The data available in the $S\bar{p}pS$-Tevatron range is not sufficient to constrain the Pomeron parameters. To overcome this problem both GLMM(08) and LKMR(09) include, in addition to the exchanged Pomeron, also secondary Regge exchanges. This enables them to extend their models to the lower ISR energies, and compare with the abundant data available at these energies. The two groups have considered rather different data bases for their fits. We shall assess these choices in section IV. Regardless, both groups, utilizing their GW models, reproduce the elastic sectors of their data bases remarkably well, with comparable $\chi^2/d.o.f.$=0.87 and 0.83 respectively. KMR(00), who tune rather than fit their data base, obtained compatible results. The three GW models considered, fail to reproduce the diffractive cross sections.

The fitted Pomeron trajectory parameters of the above GW models are compatible:

1) The $\Delta_{I\!P}$ values obtained are very similar. GLMM(08) and LKMR(09) fit $\Delta_{I\!P} = 0.12$. KMR(00) tuned $\Delta_{I\!P} = 0.10$.

2) The above GW eikonal models find very small $\alpha'_{I\!P}$ values. GLMM(08) fitted $\alpha'_{I\!P} = 0.012$,

	$\Delta_{I\!P}$	β	$\alpha'_{I\!P}$	g_1	g_2	m_1	m_2	$\chi^2/d.o.f.$
GW	0.120	0.46	0.012 GeV^{-2}	1.27 GeV^{-1}	3.33 GeV^{-1}	0.913 GeV	0.98 GeV	0.87
GW+$I\!P$-enhanced	0.335	0.34	0.010 GeV^{-2}	5.82 GeV^{-1}	239.6 GeV^{-1}	1.54 GeV	3.06 GeV	1.00

TABLE I: Fitted parameters for GLMM(08) GW and GW+$I\!P$-enhanced models.

while LKMR(09) fit is $\alpha'_{I\!P} = 0.033$. KMR(00) have a somewhat higher $\alpha'_{I\!P} = 0.066$.
3) A good reproduction of $\frac{d\sigma_{el}}{dt}$, where $t \leq 0.5GeV^2$, has been attained by all GW models we have discussed. As we shall see in the next section, the same good reproduction of $\frac{d\sigma_{el}}{dt}$ is also obtained in GW+$I\!P$-enhanced models. We shall discuss in what follows the consequences of this observation.

III. MULTI POMERON INTERACTIONS

The triple Regge diagram, leading to high mass soft diffraction, was introduced[11] almost 40 years ago. CDF analysis[13] suggests that $g_{3I\!P}$, the triple Pomeron coupling, is reasonably large. Once we assume that $g_{3I\!P}$ is not negligible, we also need to consider more complicated configurations of multi Pomeron interactions. This is the basis for the construction of the Pomeron-enhanced contributions which are consistent with t-channel unitarity. Note that these, non GW contributions, are contained in $G^{in}_{i,k}$, rather than within the GW $A^S_{i,k}$ amplitudes. As such, these calculations have to take into account the relevant unitarity suppressions expressed in terms of the corresponding survival probabilities. This study is of fundamental importance for a theoretical understanding of the Pomeron, hopefully leading to more precise predictions of the asymptotic behaviour of the scattering amplitudes.

KMR(07,08) approach is based on Ref.[9], which is derived from the Reggeon field calculus[10] with a strong emphasis on its parton model interpretation. LKMR(09) is a much simpler model where Pomeron enhancement is reduced to the zero order triple Regge approximation[11] for SD. DD is not discussed in this model. As a consequence, the tuned values of $\Delta_{I\!P}$ in the two models are very different, see Table II. In a Regge approach, such as the above, the soft Pomeron is a simple J-pole and the calculations of its interactions are non perturbative. The hard Pomeron is a branch cut in the J-plane which is treated perturbatively. Note that, in such a scheme, the hard Pomeron couplings are not necessarily factorisable. Hard Pomeron coupling factorization is assumed, though, in most eikonal

models dealing with hard diffraction.

KMR(07,08) enhanced Pomeron formalism is based on two *ad hoc* assumptions:
1) The point coupling of a multi Pomeron vertex, $n\mathbb{P} \rightarrow m\mathbb{P}$, is

$$g_m^n \,=\, \frac{1}{2}\, g_N \; nm\, \lambda^{n+m-2} \,=\, \frac{1}{2}\, nm\, g_{3\mathbb{P}}\, \lambda^{n+m-3}. \qquad \text{(III.13)}$$

In this notation $g_{3\mathbb{P}} \,=\, \lambda g_N$, where λ is a free parameter, $n + m \,>\, 2$.
2) The triple Pomeron coupling strength, is assumed to be independent of the identity (soft or hard) of the 3 coupled Pomerons.
The above two input assumptions lack any theoretical proof (see also Ref.[3]). As such, their validity depends on strong support from the accompanying data analysis. Our assessment is that the support provided to this end by KMR data analysis is inadequate (see next section).

The key input observation leading to the GLMM(08) model is the exceedingly small fitted value of $\alpha'_{\mathbb{P}}$ obtained in our GW model fit and maintained in our advanced fit based on the GW+$\mathbb{P}$-enhanced model, see Table I. The microscopic sub structure of the Pomeron is provided by Gribov's partonic interpretation of Regge theory[10], in which the slope of the Pomeron trajectory is related to $< p_t >$, the mean transverse momentum of the partons (gluons) associated with the exchanged Pomeron, $\alpha'_{\mathbb{P}} \,\propto\, 1/ < p_t >^2$. Our fitted $\alpha'_{\mathbb{P}} \,=\, 0.010$ leads to our estimate that, the typical parton momentum is large. Regardless of its intuitive appeal, the parton model is not suitable to describe gluonic interactions as it presumes a short range interaction in rapidity space, while the exchange of gluon dipoles in QCD is long range in rapidity. Recall that in pQCD the BFKL Pomeron slope approaches zero at high enough energies as $\alpha'_{\mathbb{P}} \,\propto\, 1/Q_s$. It follows that the running QCD coupling $\alpha_S \,\propto\, \pi/\ln\left(< p_t^2 > /\Lambda_{QCD}^2\right) \,\ll\, 1$, and we can consider it as our small parameter, when applying pQCD estimates to the $\mathbb{P} - \mathbb{P}$ interaction vertices.

Our pQCD motivated calculations are based on the MPSI approach[14]. Whereas KMR(07,08) assume a non zero g_m^n point coupling of $n\mathbb{P} \rightarrow m\mathbb{P}$, GLMM(08) reduce this transition to the sum of all triple Pomeron fan diagrams contributing to this configuration. In this context, partons are colourless dipoles. This construction depends on the basic one dipole splitting into two dipoles and the merging of two dipoles into one dipole, to which we assign the probabilities $P(1 \rightarrow 2)$ and $P(2 \rightarrow 1)$. For details see Refs.[2, 3].

A comparison between the Pomeron trajectory parameters obtained in GLMM(08), KMR(07), KMR(08) and LKMR(09) is presented in Table II. Our determination of $\alpha'_{\mathbb{P}}$

	GLMM(08)	KMR(07)	KMR(08)	LKMR(09)
$\Delta_{I\!P}$	0.335	0.55	0.30	0.12
$\alpha'_{I\!P}$	0.010	0	0.05	0.033

TABLE II: Pomeron trajectory parameters in $I\!P$-enhanced models.

is compatible with the KMR(07) assumption that $\alpha'_{I\!P} = 0$ and LKMR(09) and KMR(08) fits. The high $\Delta_{I\!P}$ values presented in Table II are considerably higher than conventional GW soft $\Delta_{I\!P}$, which are smaller than 0.15. These high values are compatible with BFKL and HERA high Q^2 (hard) DIS measurements. Note that there is a coupling between the fitted smallness of $\alpha'_{I\!P}$ and the large fitted value of $\Delta_{I\!P}$. The shrinkage of the forward elastic peak is a well established experimental feature. In a traditional Regge models, the shrinkage is initiated by the relatively large $\alpha'_{I\!P} = 0.25 GeV^{-2}$. Since a very small $\alpha'_{I\!P}$ is implied by all GW+$I\!P$-enhanced eikonal models, the shrinkage in these models is initiated by the unitarity screening resulting from a large $\Delta_{I\!P}$.

Our pQCD Pomeron treatment is applicable to both soft and hard Pomerons and our bare triple Pomeron coupling is, thus, universal. As such, our self consistent theoretical approach supports the KMR(07) *ad hoc* assumption on the universality of the bare $g_{3I\!P}$. As noted, the bare triple Pomeron coupling becomes smaller with energy, due to the monotonic decrease with increasing energy of the associated survival probability[15, 16].

The high $\Delta_{I\!P}$ values obtained in GLMM(08) and KMR(07,08) induce an energy dependent renormalization of $\Delta_{I\!P}$, due to Pomeron loop corrections to the input Pomeron propagator. The net result is that the effective $\Delta_{I\!P}$ is reduced with increasing energy. A schematic description of the corresponding Pomeron Green's function is given in Fig. 1. In GLMM(08,09) and this communication we have taken into account only the effect of the enhanced diagrams (Fig. 1a), and have ignored the semi-enhanced diagrams (Fig. 1b). A more complete calculation, summing over both enhanced and semi-enhanced diagram is in progress.

Technically, our calculations were executed assuming that $\alpha'_{I\!P} = 0$. This approximation implies a high energy bound of our model validity, at $W = 10^5 GeV$, which is reached when $\alpha'_{I\!P} ln(s)$ becomes significant. A similar bound was defined, also, in KMR(07,08). An additional validity bound has to be introduced so as to control the reduction of $\Delta_{I\!P}$ with energy. In general, this control is provided through higher order multi Pomeron point like

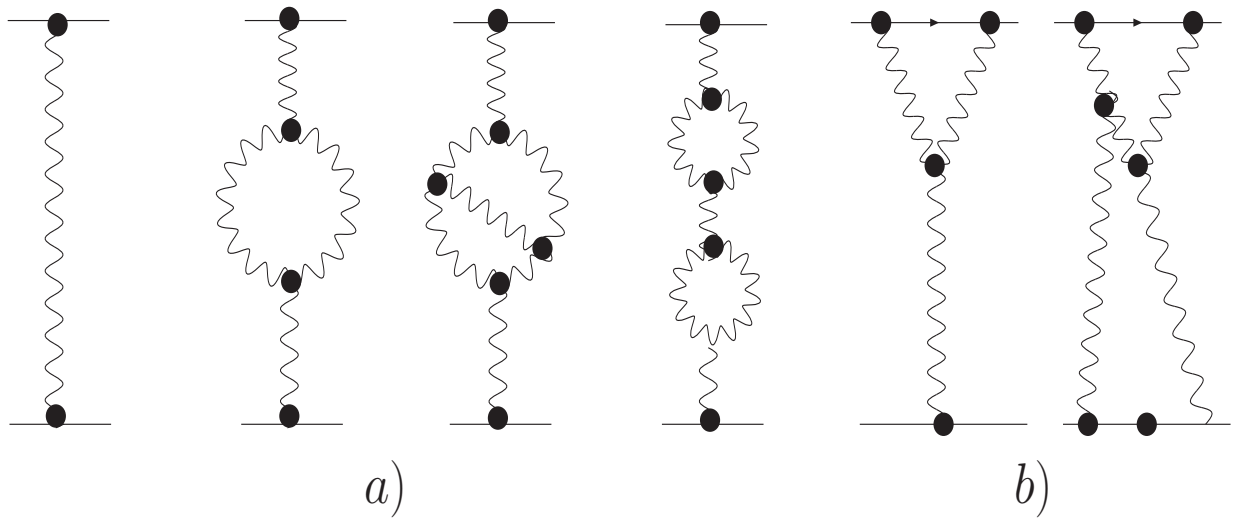

FIG. 1: Typical low order terms of the Pomeron Green's function. Enhanced Pomeron diagrams are shown in Fig. 1a, whereas Fig. 1b shows semi-enhanced diagrams which are not included in our calculations as yet.

vertices which constrain $\Delta_{I\!P}$ from becoming negative. Since our model lacks these higher order vertices, its validity has to be bound. From a practical point of view, checking Table IV in the next section, we conclude that this validity bound is higher than the bound implied by $\alpha'_{I\!P}$ and, hence, can be neglected.

IV. THE INTERPLAY BETWEEN THEORY AND DATA ANALYSIS

There is a significant difference between the data analysis carried out by the Tel Aviv and Durham groups. This is reflected in the choice of data bases made by the two groups and their procedure for determining parameters, whether be it by fitting, tuning or assuming. The starting point of both investigations is the observation that a GW model reproduces the elastic data well, but, its reproduction of the diffractive sector is deficient. Both GLMM(08), KMR(07,08) and LKMR(09) achieve an improved reproduction of their respective data bases, once the contributions of multi Pomeron diagrams are included.

The data analysis of GLMM(08) is based on a diversified data base so as to investigate simultaneously the various theoretical input elements of their model. The fitted 55 data points include the total, elastic, SD and DD soft cross sections and the elastic forward slope in the ISR-Tevatron range, to which we have added a consistency check of our predicted SD

forward slope, CDF[13] differential elastic cross sections as well as its SD mass distribution at $t = 0.05GeV^2$. The fitting of our data base was done independently twice. In the first phase for a GW model and then, again, for GW+$I\!P$-enhanced. Checking Table I, we observe that, with the exception of $\alpha'_{I\!P}$ which is very stable, the fitted Pomeron parameters of the two GLMM(08) models are different. The dramatic changes are in $\Delta_{I\!P}$ and g_2, which become much larger in the GW+$I\!P$-enhanced model. The critical observation is that, regardless of the parameters change, GLMM(08) second phase reproduction of the elastic sector is as good as its first. An example is shown in Fig. 2.

The conceptual approach of Durham group is completely different. Their data base contains just the measured values of $d\sigma_{el}/dt$, σ_{tot} and $d\sigma_{sd}/dtd(M^2/s)$ at $t = 0.05GeV^2$. LKMR(09), like KMR(00), is a two phase analysis in which the GW variables are adjusted from the elastic data and frozen to be utilized without a change in the next phase in which the triple Regge coupling is determined from the SD experimental mass distributions. KMR(07,08) do not present a GW data analysis, so we presume that theirs is a one phase GW+$I\!P$-enhanced data analysis. $\alpha'_{I\!P} = 0$ is assumed in KMR(07) and tuned in KMR(08). $\Delta_{I\!P}$ is tuned in KMR(07,08). In our opinion, Durham data base is too limited to substantiate their phenomenological goals. This may explain the shortcomings of the procedures they have adopted in their data analysis. Specifically:

1) As we saw, the features of $d\sigma_{el}/dt$ are well reproduced by all 6 models discussed in this paper, regardless of their presumed dynamics or specific parameters.

2) As demonstrated by GLMM(08), the refitted GW parameters in the GW+$I\!P$-enhanced model are significantly different (with the exception of $\alpha'_{I\!P}$) from those obtained in the GW fit. KMR models have a very simplified parametrization of the GW proton wave components. The three components differ just in their effective radii which are adjusted . This is marginally compatible with the output of GLMM(08) first phase fit, while its second phase fit requires an increase of g_2 by a factor of 60.

3) KMR(07) reproduction of CDF $d\sigma_{sd}/dtd(M^2/s)$ distributions[13] supposedly provides the support for their particular introduction of multi Pomeron interactions and the consequent tuning of $\Delta_{I\!P}$. We find this analysis inconclusive due to theoretical as well as experimental ambiguities. The extensive LKMR(09) analysis indicates the importance of triple couplings with secondary Regge contributions all through, including the highest, ISR-Tevatron energy range. This implies a significant Regge background coupled to the triple Pomeron contri-

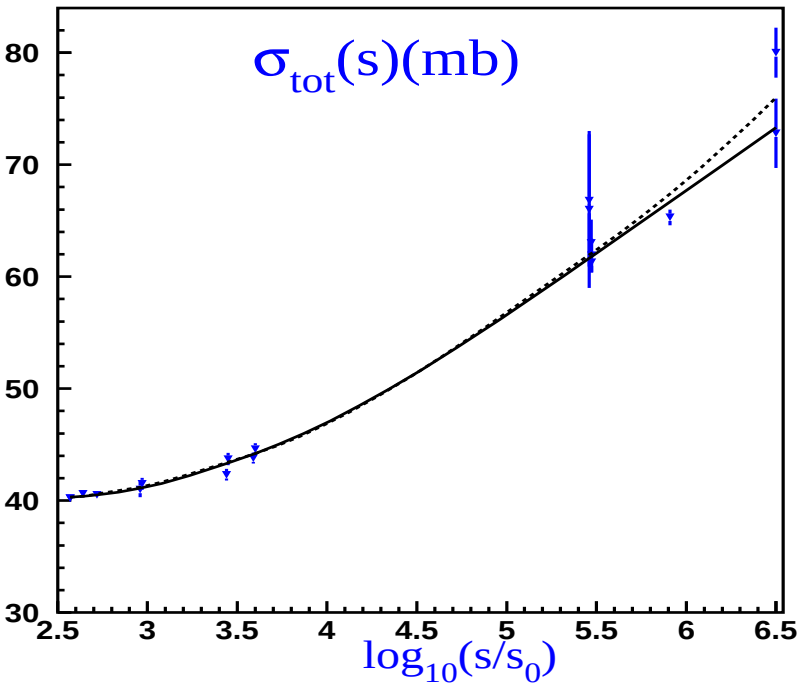

FIG. 2: Energy dependence of σ_{tot} in GLMM(08) models. Solid line corresponds to GW+$I\!P$-enhanced and dashed line to exclusive GW.

bution which is the key element of Pomeron enhancement. The less extensive analysis of KMR(07) and GLMM(08) for $d\sigma_{sd}/dtd(M^2/s)$, depends on the introduction of arbitrary background terms. Moreover, LKMR(09) noted that fitting the CDF data requires a relative rescaling of 25% between the 540 and 1800 GeV normalizations[5].

4) Ref.[4] claims a successful reproduction of the CDF high mass DD cross sections at 1800 and 630 GeV. We consider this claim not well established since the quoted data have errors of 27% and 32% respectively.

We conclude that given its meager data base, the Durham analysis does not have the resolution to determine the critical Pomeron parameters.

GLMM(08), KMR(07) and KMR(08) high energy Tevatron, LHC and Cosmic Rays predicted cross sections, as well as the survival probabilities for exclusive central diffractive Higgs production, are summarized in Table III. We have also added to the table the KMR(08) predictions for the total, elastic and SD cross sections, as well the available partial information given on the exclusive Higgs survival probability.

The elastic and total cross section predictions of the quoted models are roughly com-

	Tevatron			LHC			W=10^5 GeV		
	GLMM	KMR(07)	KMR(08)	GLMM	KMR(07)	KMR(08)	GLMM	KMR(07)	KMR(08)
σ_{tot}(mb)	73.3	74.0	73.7	92.1	88.0	91.7	108.0	98.0	108.0
σ_{el}(mb)	16.3	16.3	16.4	20.9	20.1	21.5	24.0	22.9	26.2
σ_{sd}(mb)	9.8	10.9	13.8	11.8	13.3	19.0	14.4	15.7	24.2
$\sigma_{sd}^{\text{low M}}$	8.6	4.4	4.1	10.5	5.1	4.9	12.2	5.7	5.6
$\sigma_{sd}^{\text{high M}}$	1.2	6.5	9.7	1.3	8.2	14.1	2.2	10.0	18.6
σ_{dd}(mb)	5.4	7.2		6.1	13.4		6.3	17.3	
$\frac{\sigma_{el}+\sigma_{diff}}{\sigma_{tot}}$	0.43	0.46		0.42	0.53		0.41	0.57	
S^2_{2ch}(%)	3.2	1.8-4.8		2.35	1.2-3.2		2.0	0.9-2.5	
S^2_{enh}(%)	28.5	100		6.3	100	33.3	3.3	100	
S^2(%)	0.91	2.7-4.8		0.15	1.2-3.2	1.5	0.066	0.9-2.5	

TABLE III: Comparison of GLMM, KMR(07) and KMR(08) outputs.

patible and, above the Tevatron energy, they are significantly lower than the cross sections obtained in models with no multi Pomeron contributions. This is a consequence of $\Delta_{I\!P}$ renormalization. We illustrate these features in Table IV where we present the renormalized effective values of $\Delta_{I\!P}$ in GLMM(08) and KMR(07,08) models as deduced from the corresponding cross section predictions for the Tevatron, LHC and W=10^5 GeV. Note that the values of $\Delta^{eff}_{I\!P}$ deduced from σ_{tot} and σ_{el} differ, as these cross sections are screened differently. As is evident from Table IV, this behaviour persists up to $W = 10^5 GeV$, which is the limit of validity of both the GLMM(08,09) and the KMR(07,08) calculations.

GLMM(08) and KMR(07) σ_{sd} predictions are reasonably compatible. Note, though, that the two models low and high mass diffraction contributions are inconsistent. The KMR(07) high mass diffraction grows much faster with energy than that predicted by GLMM(08). On the other hand, the GLMM(08) predictions for GW diffraction are about twice as large as those predicted by KMR(07). GLMM(08) identifies low diffractive mass with GW diffraction with no rapidity cut, whereas KMR(07,08) differentiate between low and high mass diffraction by a $\Delta y = 3$ cut. The GLMM(08,09) and the KMR(07,08) modeling of multi Pomeron interactions are fundamentally different. The large difference between their LHC diffractive predictions may serve, thus, as an effective test for the validity of the two concepts

	Tevatron → LHC			LHC → W=10^5 GeV		
	GLMM	KMR(07)	KMR(08)	GLMM	KMR(07)	KMR(08)
σ_{tot}	0.056	0.042	0.053	0.041	0.027	0.042
σ_{el}	0.030	0.026	0.033	0.018	0.017	0.025

TABLE IV: $\Delta_{I\!P}^{eff}$ values obtained from σ_{tot} and σ_{el} predictions of GLM(08)M and KMR(07,08) models.

suggested in these papers. We recall that KMR(08), which is a more advanced 3 component Pomeron model, has an even larger SD high mass diffractive cross section.

V. SURVIVAL PROBABILITIES

The experimental program at the LHC is focused, to a considerable extent, on the discovery of the Higgs boson. We shall confine our discussion to a Standard Model Higgs with a relatively low mass of 120-180 GeV, produced in an exclusive central diffraction,

$$p + p \rightarrow p + LRG + H + LRG + p. \tag{V.14}$$

The advantage of this channel is that it has a distinctive signature of two large rapidity gaps and a favorable signal to background ratio, which is improved when the forward protons are tagged.

The hard pQCD calculation of this cross section[17] is reduced due to s-channel unitarity suppressing factors, caused by the re-scatterings of the initial projectiles. We also consider the additional suppression, associated with t-channel unitarity, which is initiated by the extra screening induced by multi Pomeron interactions. The overall cross section reduction is expressed in terms of the gap survival probability which has two components shown schematically in Fig. 3,

$$S_H^2 \; = \; S_{2ch}^2 \; \times \; S_{enh}^2. \tag{V.15}$$

A detailed account of GLMM(08) S_H^2 calculations is given in Ref.[2]. The Tevatron, LHC and $W = 10^5 GeV^2$ values of the above survival probabilities are summarized in Table III. They are presented in Fig. 4 as a function of W over a wide energy range. As can be seen, the energy dependence of S_{2ch}^2 is very mild. This is compatible with the low values

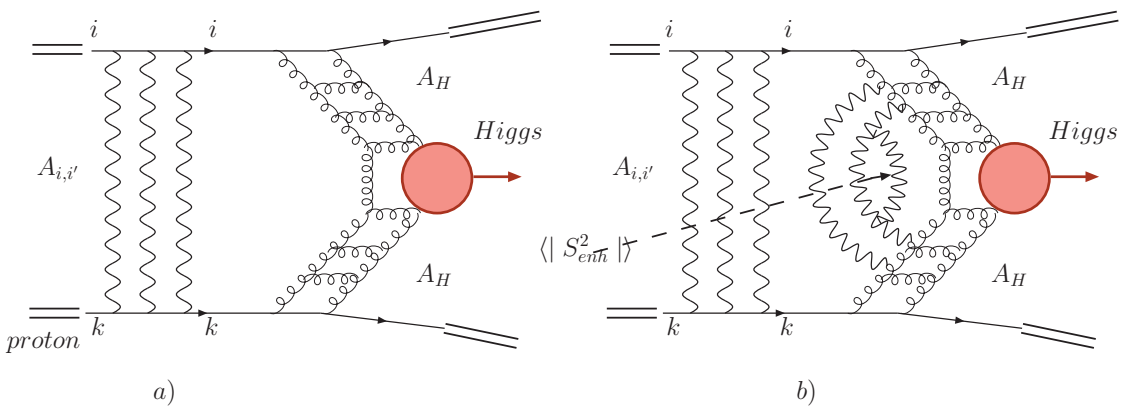

FIG. 3: Survival probability for exclusive central diffractive production of the Higgs boson. Fig. 3a shows the contribution to the survival probability from the GW two channel component. Fig. 3b illustrates an example of the additional factor S^2_{enh} initiated by multi Pomeron interactions.

of the renormalized $\Delta_{I\!P}$. Our S^2_{2ch} calculated results in the Tevatron-LHC energy range are compatible with KMR(07). Note, however, that S^2_{2ch} decrease with energy in KMR(07) estimates is somewhat faster than in GLMM(08). Hence, the difference in the reported results at $W = 10^5 GeV$ (see Table III). There is a large discrepancy between S^2_{enh} estimates given by GLMM(08) and KMR(07,08). S^2_{enh} in our model is small and has a steep energy dependence. KMR(07) do not consider this suppression, i.e. they have $S^2_{enh} = 1$. In KMR(08), $S^2_{enh} = 1/3$. The net result is that there is a large difference between GLMM(08) and KMR(07,08) estimates of S^2_H. In our calculations the decrease of S^2_H from the Tevatron to LHC is by a factor of 5-6, whereas KMR(07,08) show a much milder decrease of approximately a factor of 2.

In order to understand the difference between GLMM(08) and KMR(07,08) estimates of S^2_{enh}, we refer to the schematic Fig. 3. Assume we neglect S^2_{enh} (i.e., S^2_{enh}=1). In this case we have a "soft-hard" factorization. "Soft" relates to the soft re-scatterings of the incoming projectiles shown in Fig. 3a. "Hard" relates to the hard diffractive process. S^2_{enh} originates from three different, interfering, contributions:

1) Multi Pomeron interactions in which Pomerons from the "soft" sector interact with Pomerons from the "hard" sector. These interactions break the "soft-hard" factorization. They are included in GLMM(08,09) and KMR(08) calculations, but not in KMR(07) which neglected S^2_{enh}. KMR(08) claim that this suppression is relatively mild, at most a reduction by a factor of 3.

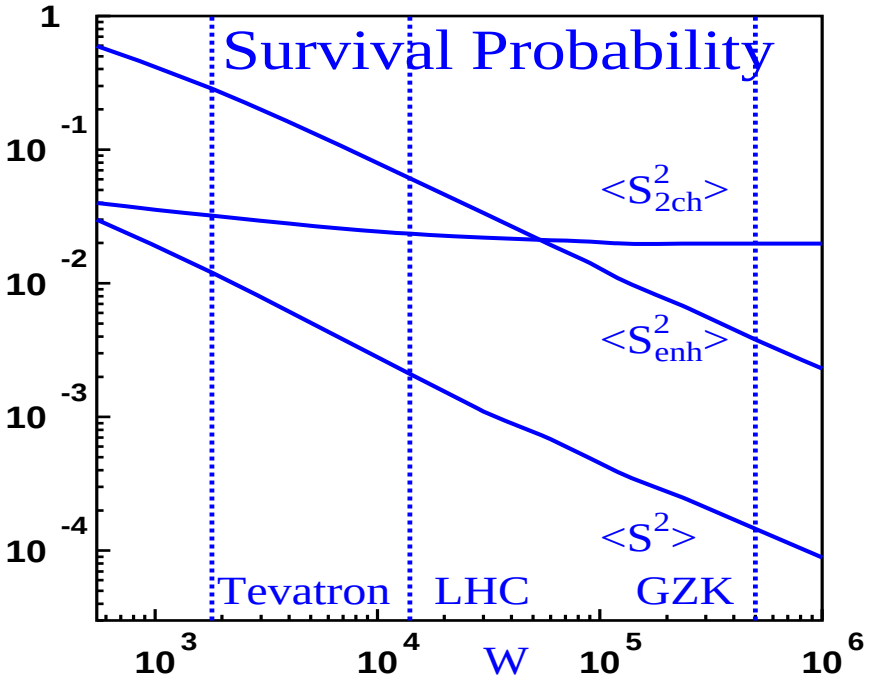

FIG. 4: Energy dependence of centrally produced Higgs survival probability.

2) Multi Pomeron interactions confined to Pomerons in the hard diffractive sector (see Fig. 3b). These interactions maintain the "soft-hard" factorization. They are included in GLMM(08,09) but not in either KMR(07) or KMR(08) estimates. In our assessment this suppression is significant.

3) Semi-enhanced Pomeron interactions are not included in either GLMM(08) or KMR(08) S^2_{enh} calculations. GLMM(09) has a calculation of S^2_{enh} in which only the semi-enhanced diagrams are included, and find its implied suppression to be significant. We are planning to finish soon a comprehensive calculation taking into account the complete set of our model's Pomerom diagrams.

VI. EXCEEDINGLY HIGH ENERGY BEHAVIOUR

The basic GW amplitudes of the GLM models are $A^S_{1,1}$, $A^S_{1,2}$ and $A^S_{2,2}$, with b dependences specified in Eq. (II.4) and Eq. (II.10). These are the building blocks with which we construct a_{el}, a_{sd} and a_{dd} (Eq. (II.6)-Eq. (II.8)). The $A^S_{i,k}$ amplitudes are bounded by the s-channel unitarity black disc bound of unity. $a_{el}(s,b)$ reaches this bound at a given (s,b) when,

and only when, $A^S_{1,1}(s,b) = A^S_{1,2}(s,b) = A^S_{2,2}(s,b) = 1$, independent of the value of β. Consequently, when $a_{el}(s,b) = 1$, $a_{sd}(s,b) = a_{dd}(s,b) = 0$.

Checking the GLMM(08) GW fitted parameters, presented in Table I, we observe that g_1 and g_2, are comparable. Indeed, the approach of $a_{el}(s, b = 0)$ to unity in GLMM(08) first phase GW model analysis, is compatible with the results obtained by KMR(07). This picture changes radically in GLMM(08) GW+$I\!P$-enhanced model in which the re-fitted $g_2 >> g_1$ are a by-product of the successful reproduction of the diffractive data base. Similar results were also obtained in a previous GW type GLM model[18], where we were able to reproduce the diffractive data only after adjusting $g_2 >> g_1$. As a consequence of the above, the three basic GW amplitudes reach the black disc bound at different energies. As g_2 is so much larger than g_1, $A^S_{2,2}(s, b = 0)$ reaches unity at a very low energy, $A^S_{1,2}(s, b = 0)$ reaches unity at approximately W=100 GeV and $A^S_{1,1}(s, b = 0)$ reaches unity at exceedingly high energies. The net result is a very slow approach of $a_{el}(s, b = 0)$ toward the black disc bound in the GLMM(08) model, reaching the bound well above the LHC energy. Recall, that the adjusted values of $A^S_{i,k}$ are determined by a fit to a GW+$I\!P$-enhanced model. Namely, a model based on both s and t-channel unitarity considerations.

The behaviour of the ratio $R_D = \frac{(\sigma_{el}+\sigma_{sd}+\sigma_{dd})}{\sigma_{tot}}$ conveys information regarding the onset of s-unitarity constraints at very high energies. Assuming that diffraction originates exclusively from the GW mechanism. We obtain, then, that the Pumplin bound[19] $R_D \leq 0.5$. The non GW multi Pomeron induced diffractive contributions are not included in this bound since they originate from $G^{in}_{i,k}$. Hence, their non screened amplitudes are suppressed by the survival probabilities which decrease with energy. The delicate balance between the increase with energy of the non screened diffractive amplitudes, and the monotonic decrease with energy of the survival probabilities, is model dependent. Indeed, the balance between these two contributions in GLMM(08) and KMR(07,08) is different. In GLMM(08), $R_D < 0.5$, decreasing very slowly with energy. In KMR(07), $R_D > 0.5$, increasing slowly with energy up to W=10^5 GeV, which is the high energy limit of validity for both KMR(07,08) and GLMM(08,09) models. The origin of the KMR(07) prediction originates from the relatively high, and fast growing, diffractive high mass cross sections coupled to a minimal decrease with energy of their S^2_{enh}, which also includes their Pomeron semi-enhanced contributions. Judging from its fast SD increase with energy, one would expect the growth of R_D in KMR(08) to be even faster. We cannot check this expectation since KMR(08) provide only

the low DD mass prediction of their model. Measurement of SD and DD cross sections at the LHC will provide crucial information on this issue.

VII. CONCLUSIONS

We conclude with our main observations:

1) Introducing multi Pomeron interactions, in addition to the conventional GW mechanism, in up-to-date eikonal models enables a reproduction of the elastic and the diffractive soft sectors.

2) We have emphasised the importance of constructing a suitable data base to test the theoretical models and determine their free parameters. In our opinion the Durham group data base is too small to reliably determine the Pomeron parameters.

3) The recent GLMM(08,09) and KMR(07,08) are contrasting models with different diagram summations. The novelty of the GLMM approach is that it correlates the smallness of the fitted $\alpha'_{I\!P}$ with the hardness of the presumed "soft Pomeron". This allows one to treat the "soft Pomeron" perturbatively. This is very different from the KMR(07,08) approach which is based on the Reggeon calculus to which KMR have added two unsubstantiated assumptions relating to the multi Pomeron couplings.

4) In GLMM(08) and KMR(07,08) the reproductions of the elastic high energy sectors are similar. Pomeron enhancement, regardless of its formulation, implies a renormalization of $\Delta_{I\!P}$. We expect, thus, the total and elastic cross sections at the LHC and Auger energies to be smaller than the non unitarised predictions.

5) There are severe differences between GLMM(08) and KMR(07) diffractive high mass predictions. The disagreement between GLMM(08) and KMR(08) is even larger. This inconsistency will probably be settled once these cross sections will be measured at the LHC.

6) The GLMM(08) and KMR(08) estimates of S^2_{enh} are very different. Both sets of calculations are not sufficiently comprehensive and need to be improved.

7) In our opinion it is misleading to assume that a model which reproduces some data or an important variable, such as a gap survival probability, at the Tevatron necessarily provides LHC predictions which are reliable. The market is full of considerably different models which claim to reproduce the Tevatron data and its deduced variables which result,

never the less, with a very wide and, sometimes, contradicting spectra of LHC predictions. Rephrasing it simply, a satisfactory comprehensive reproduction of the Tevatron data is necessary, but not sufficient to support a given model!

8) As we noted, $\Delta_{I\!P}$ is renormalized by Pomeron-enhanced dynamics. Consequently, the exceedingly high energy behaviour of a_{el}, a_{sd} and a_{dd} is determined jointly by s and t unitarity considerations. The precise asymptotic behaviour of the GW amplitudes depends not only on $g_{3I\!P}$ but also on higher multi Pomeron point couplings which are not included in the GLMM(08,09) approximations. These only become important at energies higher than 10^5 Gev (the validity bound of the model).

Acknowledgements: This research was supported in part by the Israel Science Foundation, founded by the Israeli Academy of Science and Humanities, by BSF grant # 20004019 and by a grant from Israel Ministry of Science, Culture and Sport and the Foundation for Basic Research of the Russian Federation.

---

[1] E. Gotsman, E. Levin, U. Maor, E. Naftali and A. Prygarin: *"HERA and the LHC-A workshop on the implications of HERA for LHC physics: Proceedings Part A"* (2005) 221, arXiv:hep-ph0601012.

[2] E. Gotsman, E. Levin, U. Maor and J.S. Miller: *Eur. Phys. J.* **C57** (2008) 689.

[3] E. Gotsman, E. Levin and U. Maor: arXiv:0901.1540[hep-ph].

[4] M.G. Ryskin, A.D. Martin and V.A. Khoze: *Eur. Phys. J.* **C54** (2008) 199.

[5] E.G. Luna, V.A. Khoze, A.D. Martin and M.G. Ryskin: arXiv:0807.4115[hep-ph].

[6] M.G. Ryskin, A.D. Martin and V.A. Khoze: arXiv:0812.2407[hep-ph], arXiv:0812.2414[hep-ph]; V.A. Khoze, A.D. Martin and M.G. Ryskin: arXiv:0810.3324[hep-ph], arXiv:0810.3560[hep-ph], arXiv:0810.4121[hep-ph], arXiv:0811.1481[hep-ph].

[7] M.L. Good and W.D. Walker: *Phys. Rev.* **120** (1960) 1857.

[8] E. Gotsman, E. Levin and U. Maor: *Phys. Lett.* **B452** (1999) 387, *Phys. Rev.* **D60** (1999) 094011.

[9] A.B. Kaidalov, L.A. Ponomarev and K.A. Ter-Martirosyan: *Sov. J. Nucl. Phys.* **44** (1986)

468.

[10] V. N. Gribov: arXiv:hep-ph/0006158, *Sov. J. Nucl. Phys.* **9** (1969) 369.

[11] A.H. Mueller: *Phys. Rev.* **D2** (1970) 2963, **D4** (1971) 150.

[12] V.A. Khoze, A.D. Martin and M.G. Ryskin: *Eur. Phys. J.* **C18** (2000) 167.

[13] CDF Collaboration: *Phys. Rev.* **D50** (1994) 5535; K. Goulianos and J. Montnha: *Phys. Rev.* **D59** (1999) 114017.

[14] A. H. Mueller and B. Patel: *Nucl. Phys.* **B425** (1994) 471; A. H. Mueller and G. P. Salam: *Nucl. Phys.* **B475**, (1996) 293; G. P. Salam: *Nucl. Phys.* **B461** (1996) 512; E. Iancu and A. H. Mueller: *Nucl. Phys.* **A730** (2004) 460.

[15] E. Gotsman, A. Kormilizin, E. Levin and U. Maor: *Eur. Phys. J.* **C52** (2007) 295.

[16] V.A. Khoze, A.D. Martin and M.G. Ryskin: *Phys. Lett.* **B643** (2006) 93.

[17] V.A. Khoze, A.D. Martin and M.G. Ryskin: *Eur. Phys. J.* **C23** (2002) 311.

[18] E. Gotsman, E. Levin and U. Maor: arXiv:0708.1506[hep-ph], *Braz. J. Phys.* **38** (2008) 431.

[19] J. Pumplin: *Phys. Rev.* **D8** (1973) 2.